Journal of Sedimentary Research

Journal of Sedimentary Research, 2014, v. 84, 168–182
Research Article
DOI: http://dx.doi.org/10.2110/jsr.2014.10

GROWTH PATTERNS OF SUBAQUEOUS DEPOSITIONAL CHANNEL LOBE SYSTEMS DEVELOPED OVER A BASEMENT WITH A DOWNDIP BREAK IN SLOPE: LABORATORY EXPERIMENTS

ROCIO LUZ FERNANDEZ,[1] ALESSANDRO CANTELLI,[2] CARLOS PIRMEZ,[2] OCTAVIO SEQUEIROS,[3] AND GARY PARKER[4]

[1]*National Scientific and Technical Research Council (CONICET), Universidad Nacional de Cordoba, 1611 Velez Sarsfield, Cordoba 5000, Argentina*
[2]*Shell International Exploration and Production, 3737 Bellaire Boulevard, Houston, Texas 77025, U.S.A.*
[3]*Shell International Exploration and Production B.V., Kessler Park 1, Rijswijk 2288 GS, The Netherlands*
[4]*Department of Civil & Environmental Engineering and Department of Geology, University of Illinois Urbana, Illinois 61801, U.S.A.*
e-mail: rocioluz@efn.uncor.edu

ABSTRACT: **A series of large-scale experiments on nonchannelized, depositional turbidity currents show the evolution and complex stratigraphy of channel–lobe systems developed updip and downdip of a break in slope. Two different sets of experimental turbidity currents with different sediment concentrations were run. The results provided a comparative picture of the gross structure of the fans, with information on their surfaces, growth sequences, and times of activity of the incised channels and lobed features. In particular, data analysis focused on: (a) velocity and suspended-sediment concentration of the flows themselves; (b) time and spatial sequences of channel and lobe construction and modification, and (c) spatial trends in grain-size distribution along the deposit. Significantly, the floor geometry employed in this study allowed investigation of adjustments in deep-sea fan deposition associated with natural changes in bed slope. We show here that the break in slope played a very important role in governing channel aggradation and lobe architecture over the deposit. More specifically, the slope break tended to break up the formation of long channels and enhance the formation of lobate features. A comparison with field submarine lobe analogs demonstrates that the morphodynamics and stratigraphy associated with lobed fans can indeed be modeled, within limits, at laboratory scale.**

INTRODUCTION

Subaqueous sediment-laden flows are nonconservative in that sediment can be exchanged with the erodible bed by erosion and deposition, providing the mechanism for the development of deep-sea fan features. Overall, the shape of such depositional fans reflects the importance of turbidity currents in redistributing sediment brought to the fan by channelized turbidity flows. It has been pointed out by many researchers that many deep-sea fans are not simply sheets of sediment deposited from overriding turbidity currents, but rather show an intricate pattern of channelization together with lobe migration and aggradation (Pirmez 1994; Ouchi et al. 1995; Imran et al. 2002; Yu et al. 2006).

Only during the last decade has research included the physical modeling of channelized submarine deposits created by the passage of turbidity currents (Métivier et al. 2005; Yu et al. 2006; Cantelli et al. 2011). In particular, the experiments performed by Yu et al. (2006) in a basin 2 m wide and 2.5 m long demonstrated that under the right conditions a turbidity current flowing over and depositing on an unconfined sloping surface spontaneously creates a series of leveed channels. These experimental features showed a notable resemblance to similar channels seen at the distal ends of some submarine fans. Motivated by the early experimental observations reported in Yu et al. (2006), the experiments performed more recently by Cantelli et al. (2011) documented in more detail both the dynamic evolution of the subaqueous channels and the stratigraphy created by the passage of repeated turbidity currents. The experimental knowledge gained to date on the dynamics of sediment gravity flows, channelized or otherwise, have been used extensively by modelers to propose mechanisms of channel incision and meandering in the submarine environment (Imran et al. 1998; Parsons et al. 2002; Baas et al. 2004; Métivier et al. 2005; Yu et al. 2006).

Flow structure within turbidity currents, as well as deposition from them, is expected to be greatly affected by the bed topography of the antecedent basin floor, or that created by a previous deposit. Hence, any change in the sediment load may modify the driving force of such flows. Accordingly, a downdip break in the slope of the deep-sea floor can be expected to greatly influence both deposit architecture and runout distances of such turbidity currents. Thus, in response to variations in bed gradient, subaqueous fans may display zones of rapid stacking associated with the formation of multiple fan lobes. These depositional lobes are fundamental components in most submarine fan deposits, and their morphology, stratigraphy, and vertical connectivity characteristics reflect the nature of sedimentary processes active on the fan. Allogenic controls may influence the sediment supply into the basin and the distance to which lobes can deposit into the basin, while autogenic controls may influence the lateral extent and the runout distance of the lobes, as well as the direction of their deposition, i.e., lobe switching the influence of pre-existing lobes on lobe switching (see Neethling 2009).

The effect of a slope break on the dynamics and deposits of turbidity currents has been studied by Mulder and Alexander (2001) and Gray et al. (2005). In this paper, we investigate how a break in slope influences the morphodynamic and stratigraphic evolution of channel–lobe systems emplaced by turbidity currents. First, two different rates of suspended sediment supply were explored: fans constructed by turbidity currents

Published Online: March 2014
 1527-1404/14/084-168/$03.00

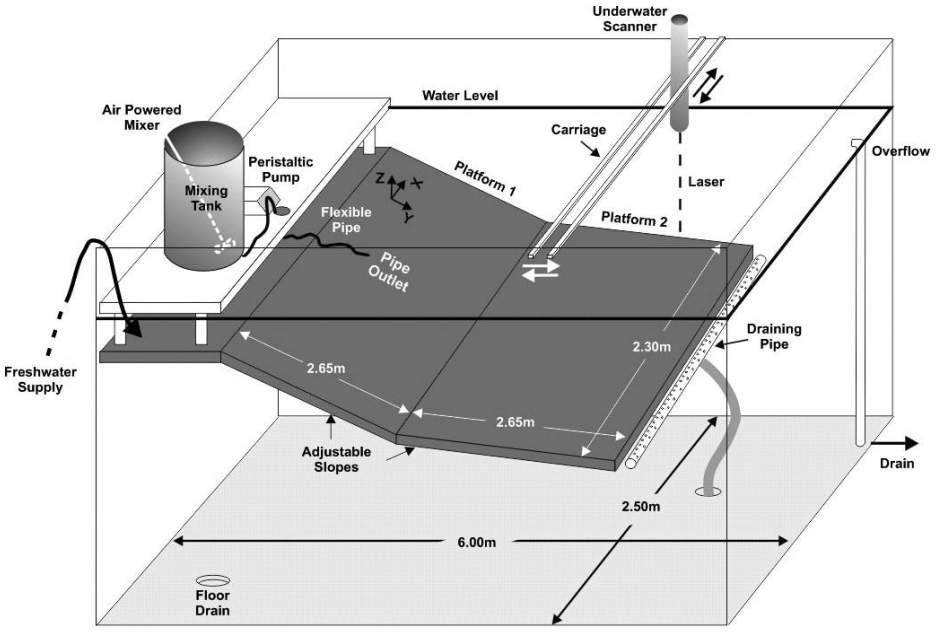

FIG. 1.—Sketch of the experimental facility in the Ven Te Chow Laboratory at the University of Illinois. The large reservoir is 6.0 m long, 2.5 m wide, and 2.5 m deep. The updip platform was set to a slope of 0.07 for all the experiments, while the slope of the downdip platform varied between the experiments.

originating from a mixture containing about 5% sediment volume concentration (low-density currents or *Experiment I*) were contrasted with deposits formed with suspension flows with a concentration of 10% (high-density currents or *Experiment II*). Second, the resulting fan morphologies were compared with the deposit of a complementary set of runs, *Experiment I-a*, which was carried out with the same release characteristics as *Experiment I*, i.e., flow rate, sediment concentration, gradation, and number of runs, but with a different set-up for the downdip platform to delineate the break in slope. Overall, the present laboratory results provide insight into the depositional processes and the controls on the dimensions, geometry, and connectivity of the deposits emplaced by turbidity currents along a break in slope.

EXPERIMENTS

Experimental Setup

The experiments were conducted in a large reservoir that was 6.0 m long, 2.5 m wide, and 2.5 m deep (Fig. 1). This tank contained two slope-adjustable steel platforms with a length of 2.65 m and a width of 2.30 m each, allowing the setting of a break in slope along an inerodible basement. In the present work, the slope of the updip platform was set to 0.070, with an abrupt change to one of two different gentler slopes of the downdip platform (Table 1).

The tank was filled with tap water to a depth of 2 m; this depth ensured that the upstream end of the updip steel platform was submerged under 0.18 m of water. During the experiments, the turbid water flowing over and off the downdip end of the downdip platform was removed by a floor drain, as well as a perforated pipe manifold set along the downstream end of the downdip platform. To maintain a constant water level, fresh water was added at the water surface in one corner of the tank, while constant depth was ensured by the presence of an overflow standpipe.

TABLE 1.—*Main differences among the experiments included in this paper.*

Experiment	Bed Slope		C_{total} %
	Updip	Downdip	
I	0.07	0.025	5
II	0.07	0.025	10
I-a	0.07	0.044	5
Cantelli et al. (2011)	0.07	0.07	10

The progress of experimentation was recorded continuously using five digital video cameras, and the density of the flow (and thus suspended-sediment concentration) was determined by sampling via siphon at various locations along the fan.

At the completion of each experiment, the reservoir was drained so as to dry the deposit; draining was sufficiently slow to avoid remobilization of sediment. The dried deposit was then sampled at different sections to examine the sediment size gradation characteristics. A laser particle sizer was used to determine grain-size distributions of the sediment samples.

Release Mechanism

A well-mixed slurry of cohesive and noncohesive sediment was prepared in a mixing reservoir of capacity 0.18 m^3 located at the upstream end of the main tank (Fig. 1). A peristaltic pump was used to drive the water–sediment mixture from the mixing tank into the main reservoir, so that flow rate and sediment concentration were kept controlled and nearly constant during experiments. The supply pipe was 9 mm in diameter; it introduced the suspended sediment onto the bed at the center of the updip platform.

The results of three experiments are reported here. Each experiment consisted of a series of flow events, here called "runs." In each run, the current was allowed to flow over the antecedent bed, so creating a stacked deposit. The number of runs and the experimental conditions for *Experiments I* and *II* are summarized in Table 2. The main difference between these two experiments was the volume concentration of the sediment–water mixture fed into the tank: it was 5% for *Experiment I* and 10% for *Experiment II*. *Experiment I-a* used the same sediment concentration and the same number of runs as *Experiment I*, but the downdip platform was set to be steeper, to 0.044.

In all cases the solid component of the slurry was composed of kaolin–silica sediments. The median grain size of the kaolin clay (K), was d_{50} = 5 μm, and the median grain sizes of the two silica flours were d_{50} = 20 μm (S20) and d_{50} = 45 μm (S45). Note that the fractions of each of the three types of sediments varied from run to run. This was done intentionally in order to encourage the development of stratigraphic

TABLE 2.—*Initial experimental conditions for the low- and high-concentration turbidity currents.*

	Experiment I and I-a: C ~ 5%		Experiment II: C ~ 10%	
Run	Released volume, m^3	Mixture K:S20:S45	Released volume, m^3	Mixture K:S20:S45
A	0.076	45:40:15	0.095	40:50:10
B	0.095	50:50:00	0.095	50:50:00
C	0.076	50:50:00	0.076	50:40:10
D	0.076	40:50:10	0.076	30:50:10
E	0.057	50:40:10	0.076	45:50:05
F	0.095	50:50:00	0.095	45:50:05
G	0.057	50:50:00	0.095	50:50:00
H	0.076	50:50:00	0.076	50:45:05
I	0.095	50:40:10	0.095	50:40:10
J			0.076	50:45:05
K			0.095	50:40:10

variation. The percentages of kaolin, S20 silica, and S45 silica fell within the following respective ranges: 30–50, 40–50, and 0–15. A complete experiment consisted of about 12 hours of flow, and involved the introduction of approximately 100 kg of sediment.

The inflow rate of the sediment–water mixture was kept constant at 1 l/min for all the experiments. This discharge ensured a well-defined turbidity current that could cover no more than a fraction of the platform at any given instant, and so that the focus of flow migrated or avulsed repeatedly across the fan surface. Such flow dynamics have been observed in previous experiments to instigate the formation of subaqueous channels (see Yu et al. 2006 and Cantelli et al. 2011), and was reproduced in the present trials.

As released at the inlet, the suspension was a relatively high-concentration slurry, with a volume concentration of either 0.05 (*Experiments I* and *I-a*) or 0.10 (*Experiment II*). Substantial dilution occurred, however, over a very short distance from the inlet, so that the current downstream could be unambiguously described as a turbidity current. Figure 2 documents this dilution process (displayed as concentrations within the current as fractions of inlet concentration C_i) for the case of *Experiment I*. Figure 2A indicates a volume suspended-sediment concentration of about 0.00275 less than 0.25 m downstream of the discharge point, with continued decrease farther downstream. High turbulence at the interface between the underflow and the ambient water above induced a high rate of entrainment of ambient water there, so resulting in dilution to a turbidity current over a short fraction of the study reach of 5.3 m. Figure 2A also illustrates the propagation of the turbidity-current front (solid lines) at intervals of $\Delta t = 10$ seconds shortly after the commencement of *Experiment I*. Velocities of the nonchannelized turbidity current varied thus from 0.07 m/s near the inlet to less than 0.01 m/s along the downdip platform. Also, the flow velocities were highest along the central flow axis and lowest at the outer margins of the current.

Data Acquisition with Underwater Scanner

Before and after each turbidity-current event, here termed a run, the topography of the steel basement or antecedent sedimentary deposit was measured using a self-positioning underwater laser system scanner. Data collected by the triangulating distance sensor of the device was logged onto a computer. A stepper motor ensured movement of the system along the longitudinal and transverse directions (see Fig. 1). The instrument had a sampling frequency of 100,000 Hz and an accuracy of 1/10 mm. In all the experiments, data acquisition was implemented at 0.02 m intervals in the downstream direction and 0.001 m in the transverse direction.

EXPERIMENT I: DEPOSITIONAL TRENDS

The depositional history of the deposit in *Experiment I* as obtained from the laser scanner is shown in Figure 3. Each panel in that figure represents the bed topography at the end of each run, all of which are shown therein. Alternatively, Figure 4 displays photomosaics of the entire fan surface for six of the nice runs of this experiment. The occasional introduction of dye during the experiment helped document the channels visible in the panels of Figure 4. Figures 3 and 4 provide a complete documentation of fan evolution, including the formation and shifting of channels and depositional lobes and the response of the fan and its channels to the slope break.

At the very beginning of the experiment, a fan started to develop downslope without distinct channels on the surface of the deposit. This is illustrated in Figure 3A, which shows the bed topography at the end of Run A. By the end of Run B (Figs. 3B, 4A), the flow had started to confine itself, and newly developed leveed channels became visible along the fan (C1 and C2 in Fig. 3B, for example). All the topography shown in Figure 3A and B and Figure 4A was aggradational in nature.

As expected, it was observed during the experiment that flows tended to be confined to pre-existing channels for some time. Occasionally, several channels became infilled (e.g., C1 and C2, which are well-defined in Figures 3B and 4A pertaining to Run B, but difficult to discern in Figures 3C and 4B pertaining to Run C), after which the flow became divided once more into various new distributaries and other pre-existing channels (e.g., C3–C5 in Figure 3C and D pertaining to Runs C and D, respectively).

Toward the end of *Experiment I*, the abrupt break in the slope had been greatly subdued by sediment deposition, but it was still evident in the depositional morphology of the deposit (see Figures 3H and 4C pertaining to Run H), in terms of well-defined semicircular, poorly channelized lobes beyond the initial break. The basement slope break shown in Figure 1 is thus seen to have substantially influenced the overall morphology of the deposit, with sediment lobes being the most common feature on the downdip platform.

The overall surface of the deposit thus showed three recognizable morphologic divisions, which can be seen in Figure 3H for Run I: (a) a steep sediment supply area defining the source zone of the fan; (b) a middle fan zone characterized by leveed channels; and (c) a lower zone beyond the basement slope break which was free of major channels, instead consisting of stacked depositional lobes. These three observed fan divisions are documented in more detail below.

Source Zone: the Control on Flow Properties Near the Sediment Input

Over time, much of the released mixture deposited in a short zone proximal to the pipe outlet, here called the source zone, so as to form a small but prominent cone of accumulated sediment with a radius in the range 0.1–0.2 m (see Fig. 3). A small depression formed at the top of this cone, where the flow exited from a flexible pipe which brought it from the mixing tank into the large reservoir of Figure 1. The cone of about 8 cm high and depression are apparent in Figure 3B (corresponding to Run B) showing the topography, and the depression is also apparent in the photomosaic of Figure 4B corresponding to Run C. While the depression and cone are not representative of the upstream end of a typical submarine fan, they nevertheless provided an excellent way to dilute the incoming slurry, so that it evolved into a much more dilute turbidity current not far downstream (see Yu et al. 2006).

It is evident from Figure 3A and B that channels first started to appear during Run B. The process of channelization is documented in Figure 5, which shows the flow at four different times during the early stages of Run B. The turbidity currents in Figure 5 flow down the cone after overflowing the rim of the depression. Because the sediment size ranges in the slurry were not in equilibrium with the basement, coarser material was

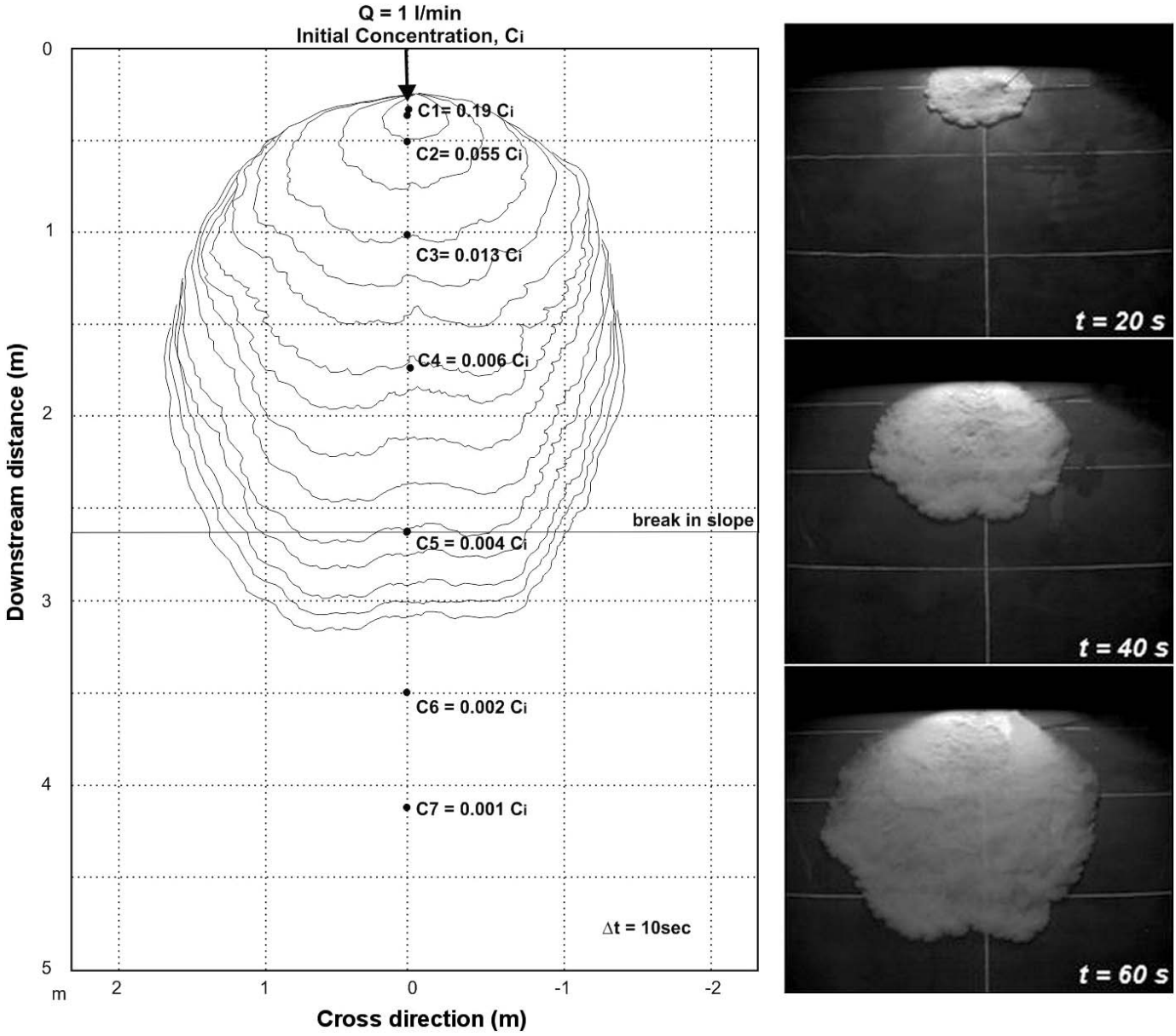

FIG. 2.—Line drawing of flow-front positions and dilution of the nonchannelized turbidity current during its propagation along the platforms (Run A of *Experiment I*). Plan-view dimensions of steel platforms are also shown. Photos on the right show different flow-front positions.

deposited within the cone as the flow adjusted downstream. More specifically, nearly all of the medium silt ($d_{50} \sim 45$ μm) and most of the fine silt ($d_{50} \sim 20$ μm) material were deposited in the cone. As documented in detail below, the cone was the coarsest zone of the deposit, with a mean sediment diameter $d_{50} \sim 32$ μm.

As suggested by the measured deposits of Figure 3A and B and the photographs of Figure 5A and B, the initially featureless deposit at the beginning of run evolved over time to a more complex topography, within which channels started to become evident (Fig. 5C, D). Along this upper area of the deposit, the average flow velocity estimated from videos by using dye as a tracer was about 0.025 m/s for the zones of unconfined flow, and within the channels it was in the range 0.04–0.07 m/s (Fig. 5).

Flow thickness was estimated to be ~ 0.01 m, based on the laboratory observations and on the previous work by Yu et al. (2006). The combination of velocity, concentration, and flow thickness allowed the estimation of the densimetric Froude number Fr_d of the flow. Here $Fr_d = U/(ghRC)^{0.5}$, where U is the average velocity of the flow, here estimated from either the velocity of the front of the turbidity current (Fig. 5A, B) or velocity in the body of the channelized flow as determined from dye (Fig. 5C, D). In addition, g is the acceleration of gravity, h is the flow thickness, C is the volume concentration of suspended sediment, and R is the submerged specific gravity of the sediment itself (~ 1.65 for quartz).

Unchannelized turbidity currents overflowed the depression with a Froude number Fr_d close to unity, and evolved downstream over a short distance to a subcritical flow with $Fr_d < 0.5$. The cone in the source area thus provided a short zone of adjustment within which (a) the flow became greatly diluted, (b) the flow regime became Froude-subcritical, and (c) coarser sizes were deposited proximally, leaving only the finer sizes to build the much longer fan extending downdip.

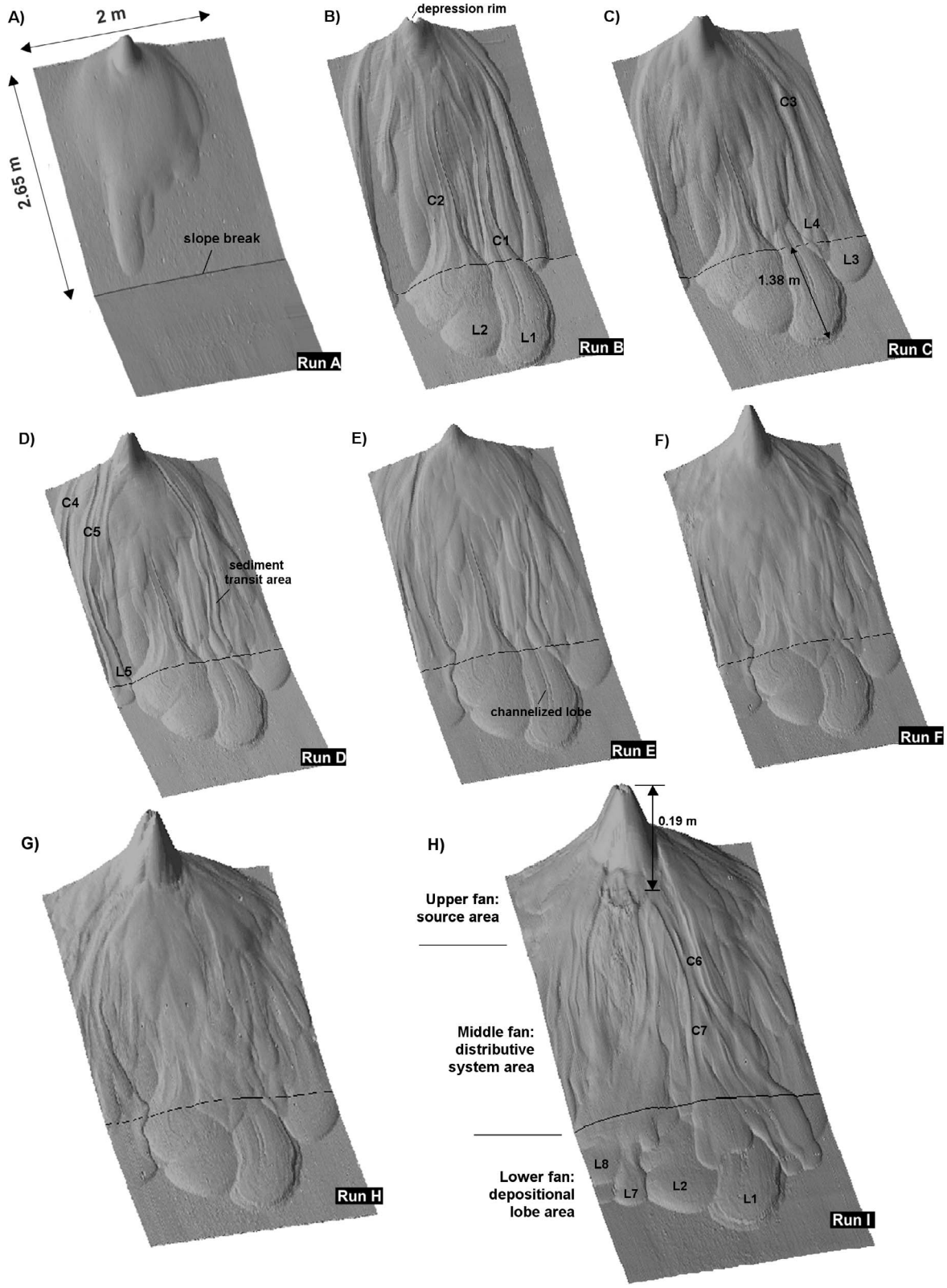

FIG. 3.—Laser-measured depositional history of the fan deposit through *Experiment I*, with vertical exaggeration. The most characteristic feature for which the break in slope was responsible was the adjustment of the flow depositional regime; at the lower slope of the downdip basin floor, the channels widened progressively and gave way to a number of lobes that formed within the deposit.

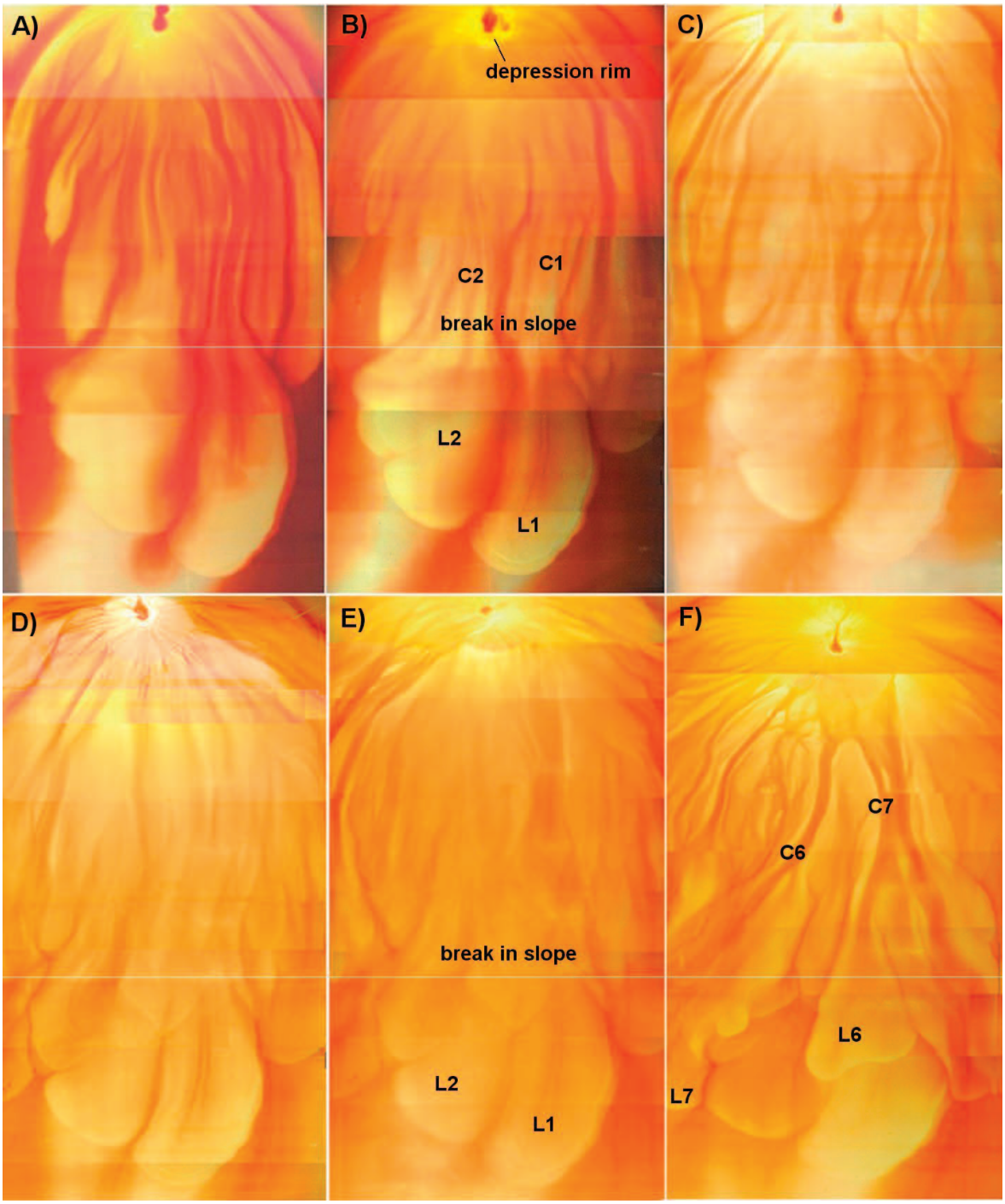

FIG. 4.—Photomosaic of the entire fan surface after the end of: **A)** Run B, **B)** Run C, **C)** Run D, **D)** Run E, **E)** Run H, and **F)** Run I, in *Experiment I*. Images show the reworking of the deposit run to run during the experiment.

The flow Reynolds number Re was computed as Uh/v, where the kinematic viscosity of water v was estimated using the value for clear water at 20°C. Based on the velocities of Figure 5, Re was within the range of 400 at the inlet, and decreased to 150 as the flow propagates along the deposits. The flows that created the channels were thus laminar, or at best weakly turbulent.

Turbidity currents at field scale are likely fully turbulent. The difference between the laboratory and field flows, however, does not invalidate the usefulness or applicability of the experiments. Indeed, Lajeunesse et al. (2010) have shown that most of the morphodynamics of rivers can be captured at laminar scale or near-laminar scale, including self-formed channels, dunes, antidunes, bars, and meandering. Even though such experiments are not precise scale models of the field, it is found that a number of features scale remarkably well. Paola et al. (2009) have remarked upon the "unreasonable effectiveness" of small-scale stratigraphic and geomorphic experiments.

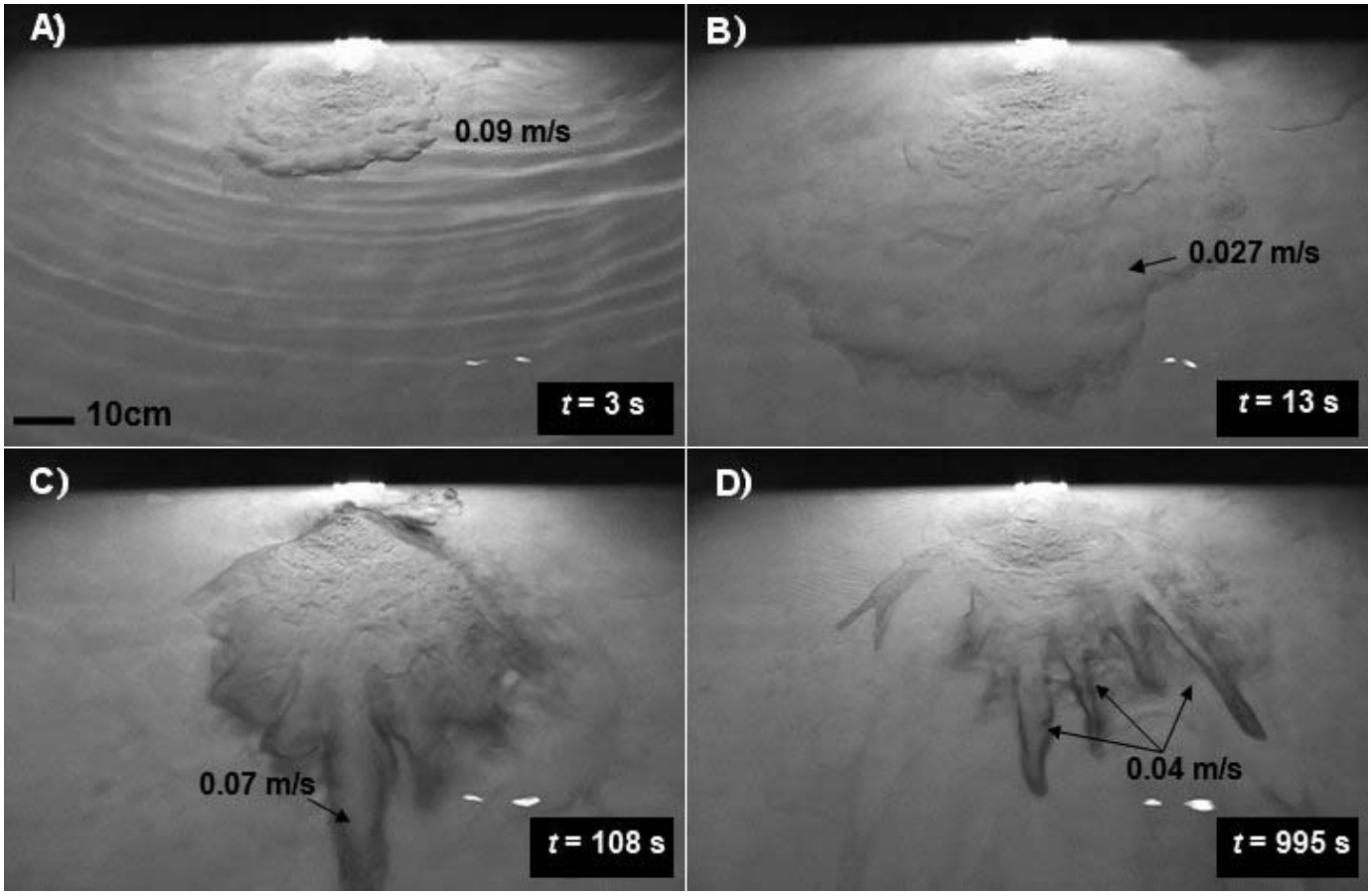

FIG. 5.—Photographs at different time intervals illustrating flow velocities during the self-channelization process near the inlet area. Photographs taken during Run B in *Experiment I*.

Middle-Fan Zone: the Distributary System

This part of the deposit was recognized as the area where a system of stacked, overlapping channels was formed (e.g., Fig. 3B). These channels tended to be differentially filled and abandoned due to aggradation, and then replaced by new channels during the following runs. Usually there were several simultaneously active channels, with one or more of this group carrying most of the flow. Figure 3B and the corresponding photo in Figure 4A suggest that the laterally central region of the central zone of the fan was the most dynamic zone. The main active channels are labeled as C1 and C2; each of these two channels ends in a lobe deposit, labeled respectively as L1 and L2. Eventually, the active channels C1 and C2 were abandoned along part or all of their courses, probably through avulsion (Figs. 3C, 4B). A new side channel C3 then developed, where bed gradients were steeper, and it gradually captured more of the flow so as to become dominant. As it did so, new channels formed (see C4 and C5 in Figs. 3D, 4C) and old channels were abandoned. This avulsion process of formation and abandonment continued to the end of the experiment, shown in Figures 3H and 4F. Hence, the succession of several channel–

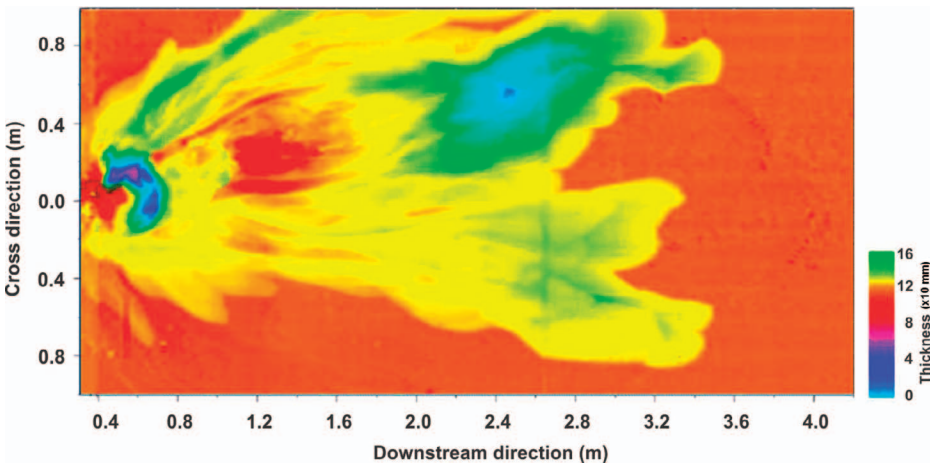

FIG. 6.—Isopach map illustrating variation of thickness within Run I in *Experiment I*. The break in slope is located at 2.65 m downstream direction.

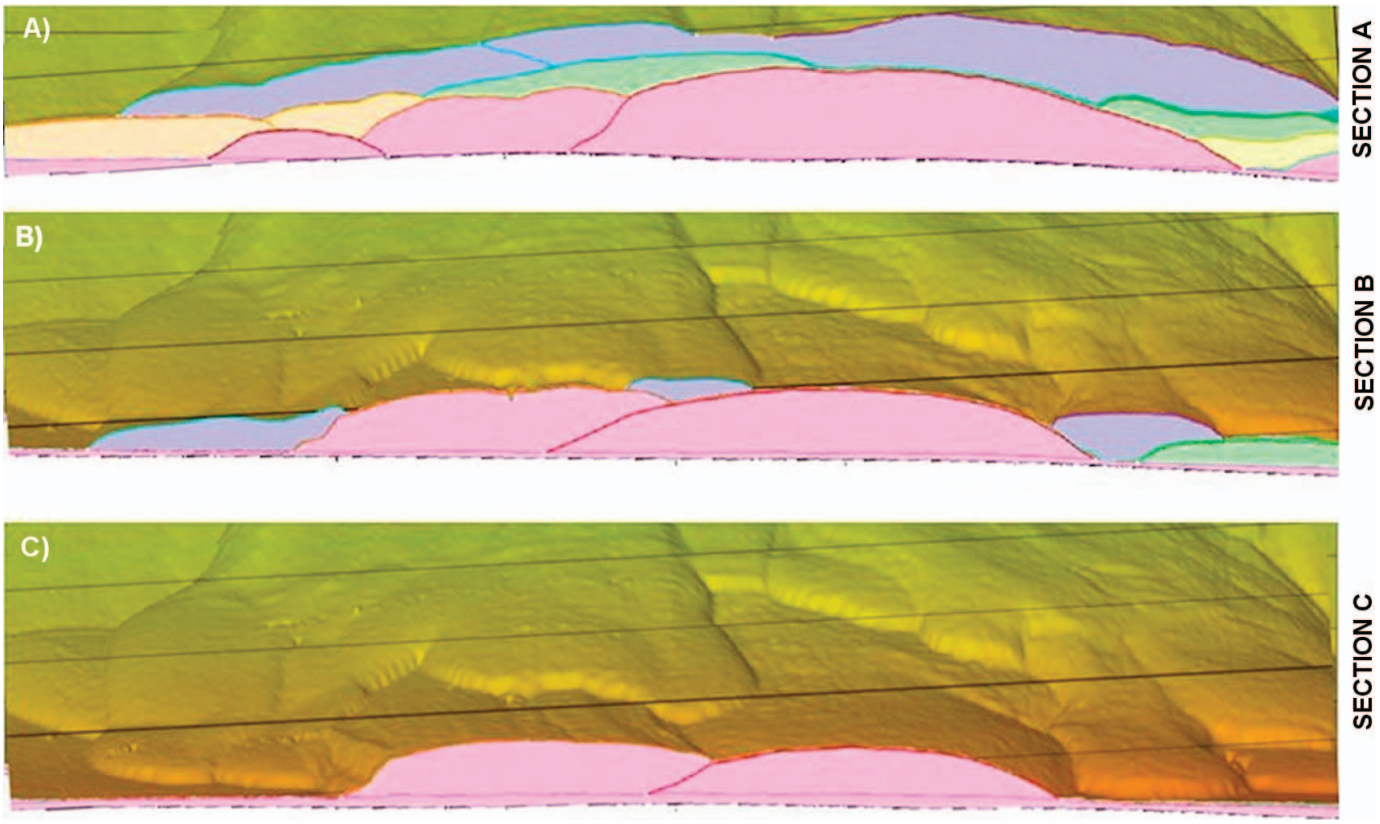

FIG. 7.—Cross section of laser scan data showing lobe deposits in *Experiment I*. Section A is located at 2.8 m, Section B at 3.2 m, and Section C at 3.6 m in accordance with Figure 6. Results suggest that lobe thickness decreased downslope during the growing up of the deposits.

levee systems that were formed and then abandoned gradually built the fan deposit upward as well as laterally as it prograded downslope.

The laboratory observations during *Experiment I* suggest thus that the deposit developed sequentially, by a process in which channels and their levees locally accumulated much faster that the average sedimentation rate for the rest of the deposit. The result was a relatively thick deposit in the distributive system of the numerous channel elements in the middle fan. This is documented in Figure 6, which is a map of total deposit thickness isopachs at the end of Run I (which also corresponds to the end of *Experiment I*). The difference in elevation between the top of the levee and the adjacent channel bed was on the order of 2–4 mm. The channel width typically ranged between 1 and 5 centimeters near the upslope end of the middle fan but tended to increase downslope.

Lower Fan Zone: Lobe

The lower-fan region is characterized by stacked lobes. The emplacement of any given lobe was related to flow deceleration, channel expansion, and resulting sediment deposition where the gradient decreased at the break in slope. The loss of sediment transport capacity at the slope break caused the emplacement of a lobe that was much wider than the source channel immediately upstream (Figs. 3, 4). All lobes were generally several centimeters wide (0.1–0.6 m) and commonly were slightly elongated in the direction of the flow (with lengths up to 1.3 m) as compared to the transverse direction. According to the depositional history of *Experiment I* shown in Figure 3 (measured with the underwater scanner) and Figure 4 (aerial view), central lobes were first to develop as bodies of sediment deposited at the channel mouths; these are labeled as L1 and L2 in Figure 3B. These structures were followed in time by the lobes formed on the margins of the platforms or experimental basin floors (lobes L3, L4, and L5 in Fig. 3C, D) and then by the new lobe system developed on the top of the antecedent ones (lobes L6, L7, and L8 of Fig. 3H).Therefore, the deposit was observed to expand first across the entire platform width and then to aggrade due to compensational stacking, with a thicker deposit near the channel center.

Figure 3H documents the process of lobe switching. Deposition just beyond the end of channel C7 caused the emplacement of lobe L6 beyond the slope break. Subsequent aggradation in the region created an unsustainably high zone, and so the feeder channel avulsed, resulting in the subsequent emplacement of lobe L7.

The final architecture observed at the end of *Experiment I* was the result of both the position and size of preexisting channels and lobes and the break in basement slope. The first of these drove the pattern of compensational stacking. The second of these controlled the change from well-developed channelization in the middle fan zone to relatively unchannelized lobes in the lower fan zone, and also accentuated the pattern of deposition near the slope break.

As the fan developed, channels occasionally became plugged with sediment as the flow traversed the break in slope. After a few runs, the channels could no longer confine the subsequent flows in this zone of the deposit. The flow then spread out below the slope break to emplace a well-distinct lobe, as illustrated in Run E of Figure 3E. Hence, each lobe was well defined, and they were stacked successively and compensationally on top of one another, as is shown in Figure 3, and even more clearly later in Figure 7. The isopach map of Figure 6 illustrates then the variation of thickness within Run I in *Experiment I*. The maximum thickness of a lobe typically occurred within 0.5 m of the break in slope. The cross sections along the downdip platform shown in Figure 7 suggest that lobe thickness decreased downslope.

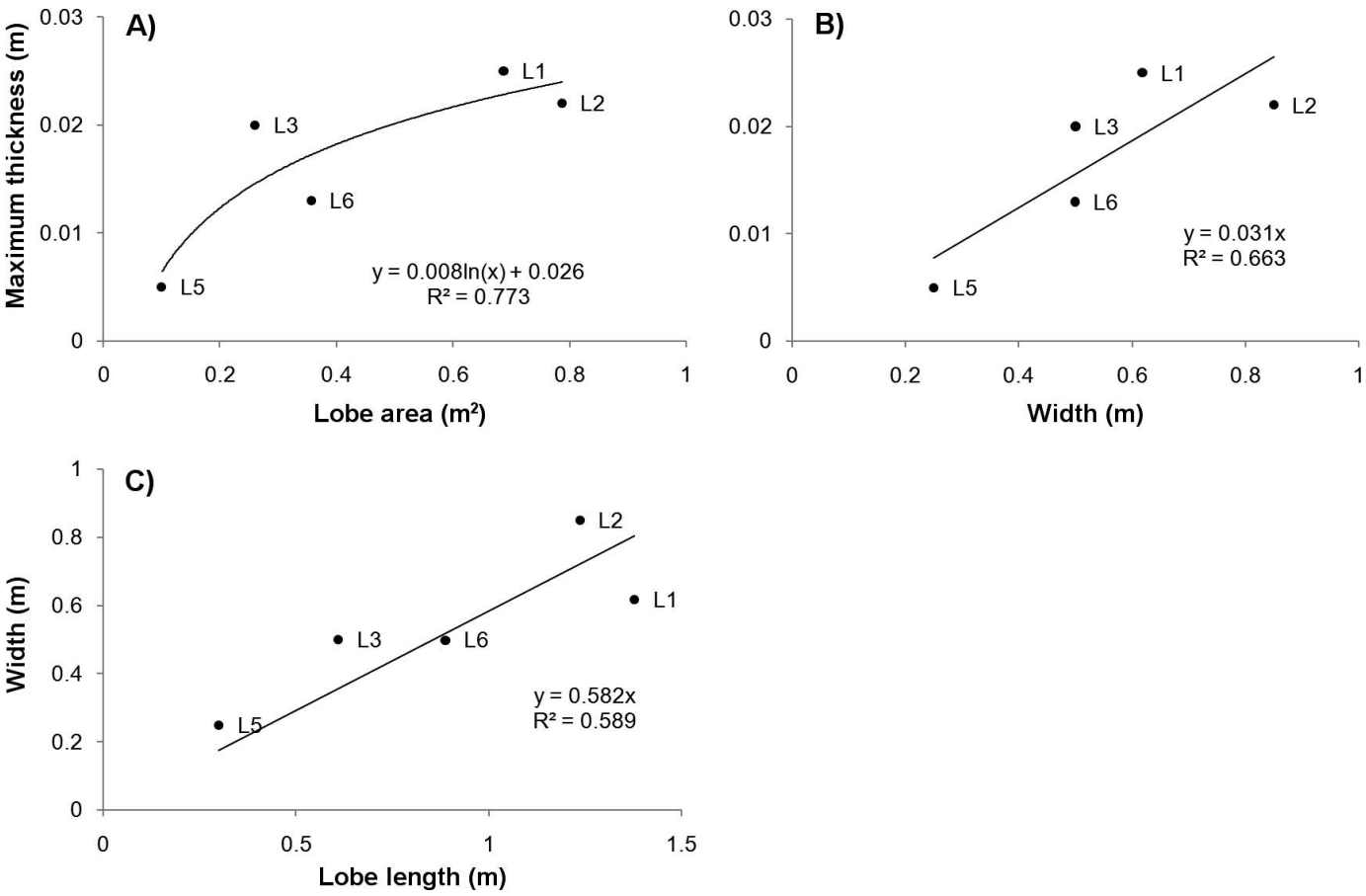

FIG. 8.—Crossplots of: **A)** maximum lobe thickness versus lobe area, **B)** maximum lobe thickness versus width, and **C)** width versus lobe length, measured in *Experiment I* deposit.

Figure 8 documents: (a) maximum lobe thickness versus lobe area, (b) maximum lobe thickness versus lobe width, and (c) lobe width versus lobe length. The figures indicate that thickness, area, length, and width are all positively correlated with each other. The observation that thicker lobes tend to be longer (Fig. 8C) is in agreement with the measurements of Deptuck et al. (2007) in natural seafloor deposits.

EXPERIMENT II: EFFECT OF VARYING INFLOW SEDIMENT CONCENTRATION

A second experiment, *Experiment II*, was performed with the same initial configuration as *Experiment I*, but with the volume sediment input concentration increased from 0.05 to 0.10. The two experiments were very similar other than the difference in input concentration. For example, it can be seen in Table 2 that *Experiment I* consisted of nine runs, whereas *Experiment II* consisted of 11 runs.

The bed topographies for the last six runs of *Experiment II* are shown in Figure 9 (with the same scale and vertical exaggeration used in Fig. 3). A comparison with Figure 3 pertaining to *Experiment I* indicates that the two experiments show similar depositional histories. For example, the distal margins of the fan lobes observed at the end of an experiment are roughly the same for both cases. In addition, intense channelization is evident in both cases. Three differences are, however, evident. The higher concentration of *Experiment II* resulted in a thicker deposit than *Experiment I* (rather than, e.g., a longer deposit of similar thickness). The topography at the end of *Experiment II* shows about twice as many distal lobes as in the case of *Experiment I*, and lobe size is correspondingly smaller. Finally, in *Experiment II*, leveed channels have formed in a very thin, sheet-like deposit downstream of the lobes; these very distal channels are absent in the case of *Experiment I*.

Figure 10 illustrates the reworking of the fan surface from Run I to Run J of *Experiment II* (see also Fig. 9). The channel denoted as C9 in Figures 9 and 10 had developed and emplaced a substantial distal lobe by the end of Run I. At some time during Run J, however, this channel was abandoned in favor of the one marked C10. This new channel had begun the process of emplacing a new lobe by the end of Run J. This cycle of channel formation, emplacement of lobes, and channel abandonment was evident during both experiments.

A comparison of Figures 3 and 9 shows another difference between *Experiment I* and *Experiment II*. By the end of *Experiment II*, the cone-shaped deposit in the source fan zone is more prominent that at the end of *Experiment I*. A doubling of the sediment input concentration evidently caused substantially more proximal deposition of coarse sediment near the inlet.

The relation between bed topography (solid line) and the mean grain size of bed sediment (circles) is shown in Figure 11 for both *Experiments I* and *II*. The line profiles shown are oriented centerline downstream; they were taken at the end of the experiments. The elevation profiles are concave upward, as might be expected in the case of a fan that is aggrading and prograding. A zone of approximately constant slope corresponding to the cone (source fan zone) is apparent at the upstream end. Five measurements for each experiment also illustrate a strong pattern of downfan fining, with mean grain size declining from around 32 μm to around 7 μm over about 3 m.

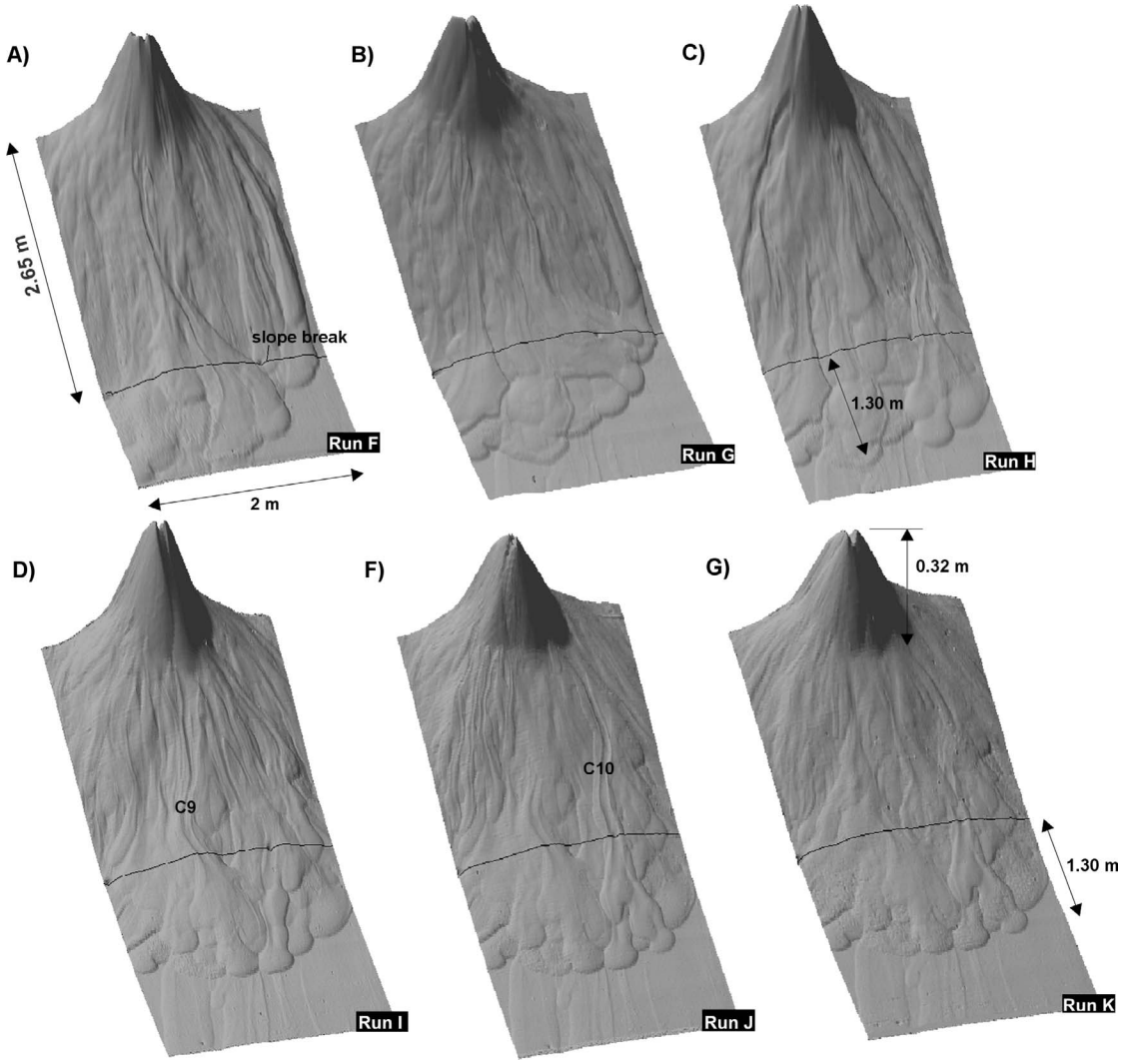

FIG. 9.—Laser-measured depositional history from Run F to Run K of the fan deposit in *Experiment II*. **A**, **B)** Multiple channels exist at this time, but the ones in the center are dominant. **C)** In Run F the marginal portion of the fan is now active. **D)** Run I, showing the active channel C9. **E)** In Run J, channel C9 is abandoned and C10 becomes dominant. **F)** Deposit after 11 hours of run.

Figure 11 also shows that most of the sediment in the coarsest component of the mix (S45; d_{50} = 45 μm) and much of the finer silica flour (S20; d_{50} = 20 μm) settled out in the cone. More specifically, mean grain size declines from 32 μm near the top of the cone to 23 μm at a point about 1 m downfan of the break in slope. Analogs to this cone-like feature were also observed in the experiments on channelized submarine fans by Yu et al. (2006) and Cantelli et al. (2011). The formation of this feature evidently allows the flow and sediment concentration to adjust so as to promote the formation of leveed channels in finer material (kaolin, K, and some of the finer grade of silica flour, S20) farther downstream.

GRAIN-SIZE VARIATION

A typical pattern of grain-size variation along the deposit is shown in more detail in Figure 12 for *Experiment I-a*, which was performed with the same release characteristics as *Experiment I*, i.e., flow rate, sediment concentration, gradation, and number of runs, but with a different set-up for the downdip platform to define break in slope (see Table 1). The fan topography at the end of *Experiment I-a* is shown in Figure 12A, and the patterns of grain size variation are shown in Figure 12B, C, and D. It should be noted that a similar pattern of grain-size distribution for the final deposit was observed for the other two experiments commented earlier in this work.

Figure 12B shows the downfan variation in grain-size distribution along the fan centerline (C in the legend) and a line to left side of centerline looking upfan (S in the legend). Also shown is the initial grain-size distribution of the sediment mix at the source. The single sample from the cone (1C) shows a very coarse distribution, with a strong bias toward the S45 silica flour; the median size is 45 μm. The only sample that more or less reflects the grain-size distribution is 1S, which corresponds to just below the slope break at the base of the cone. All of the other grain-size distributions show median sizes below 10 μm. The samples show downfan fining, mostly through a tendency for the coarser half of each distribution to become finer. Samples 2C–5C along the centerline and 2S–5S along the side show similar fining trends.

In Figure 12C, a single channel is followed downstream. Samples 1T–4T correspond to channel thalweg, ordered from upstream to downstream. Samples 1L–4L correspond to channel levee adjacent to the corresponding

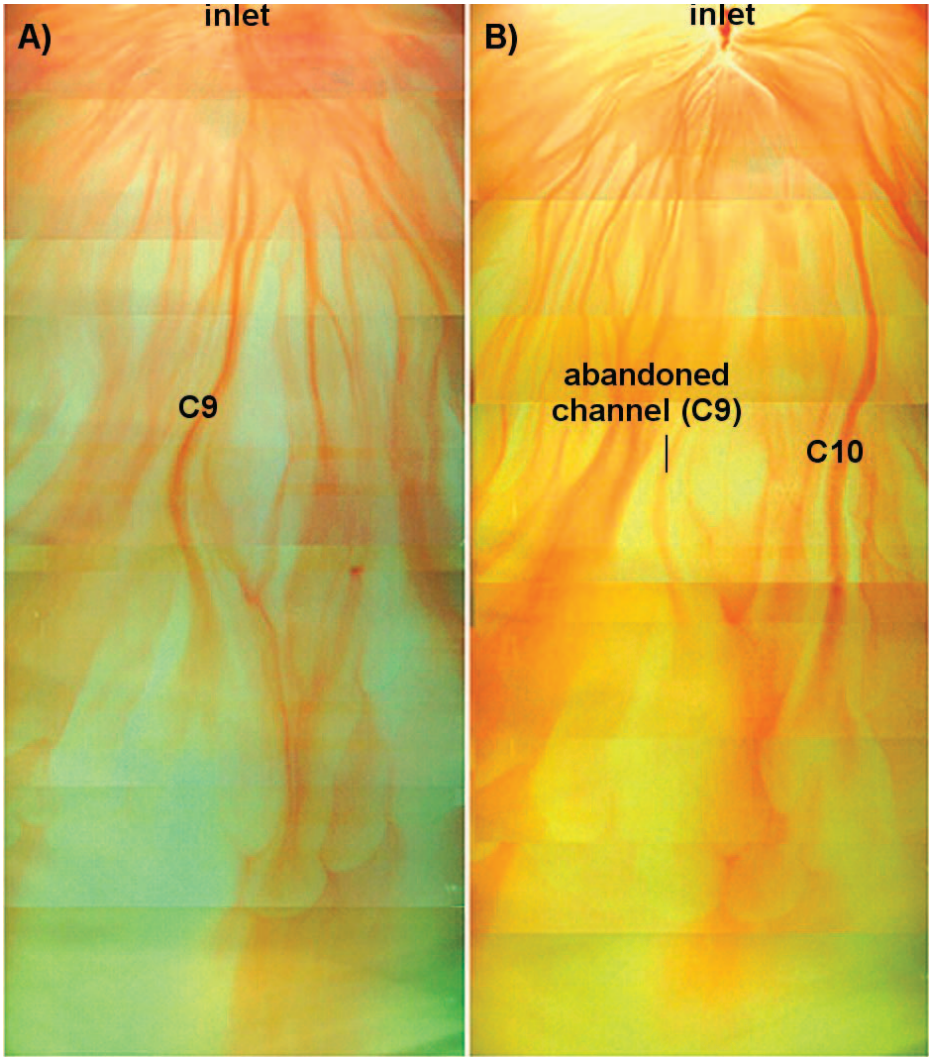

FIG. 10.—Aerial view (photomosaic) of the entire fan showing the reworking of the fan surface from **A)** Run I to **B)** Run J, during *Experiment II*. Average width of indicated channels is 0.04 m.

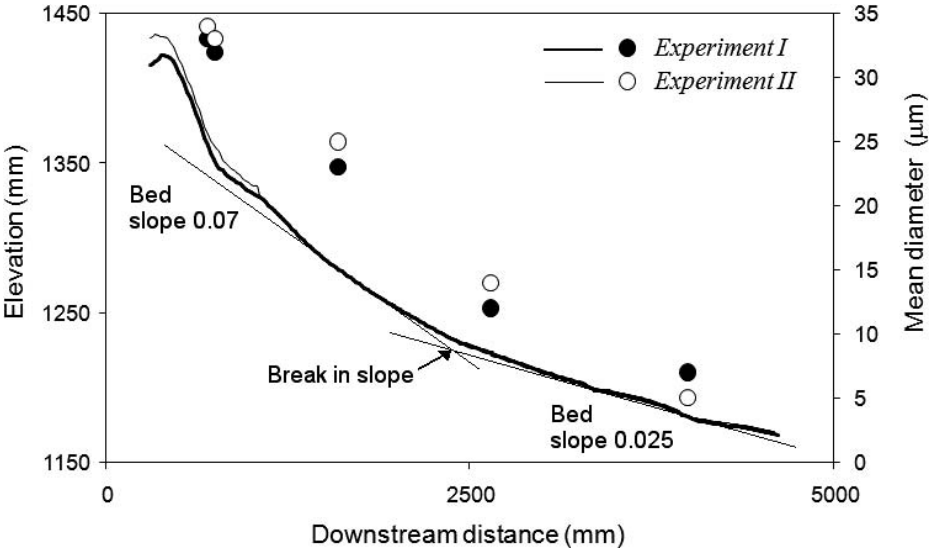

FIG. 11.—Bed elevation for *Experiment I* and *Experiment II*, illustrating the concave- upward longitudinal profile and downstream fining along the deposits. Flow was from left to right.

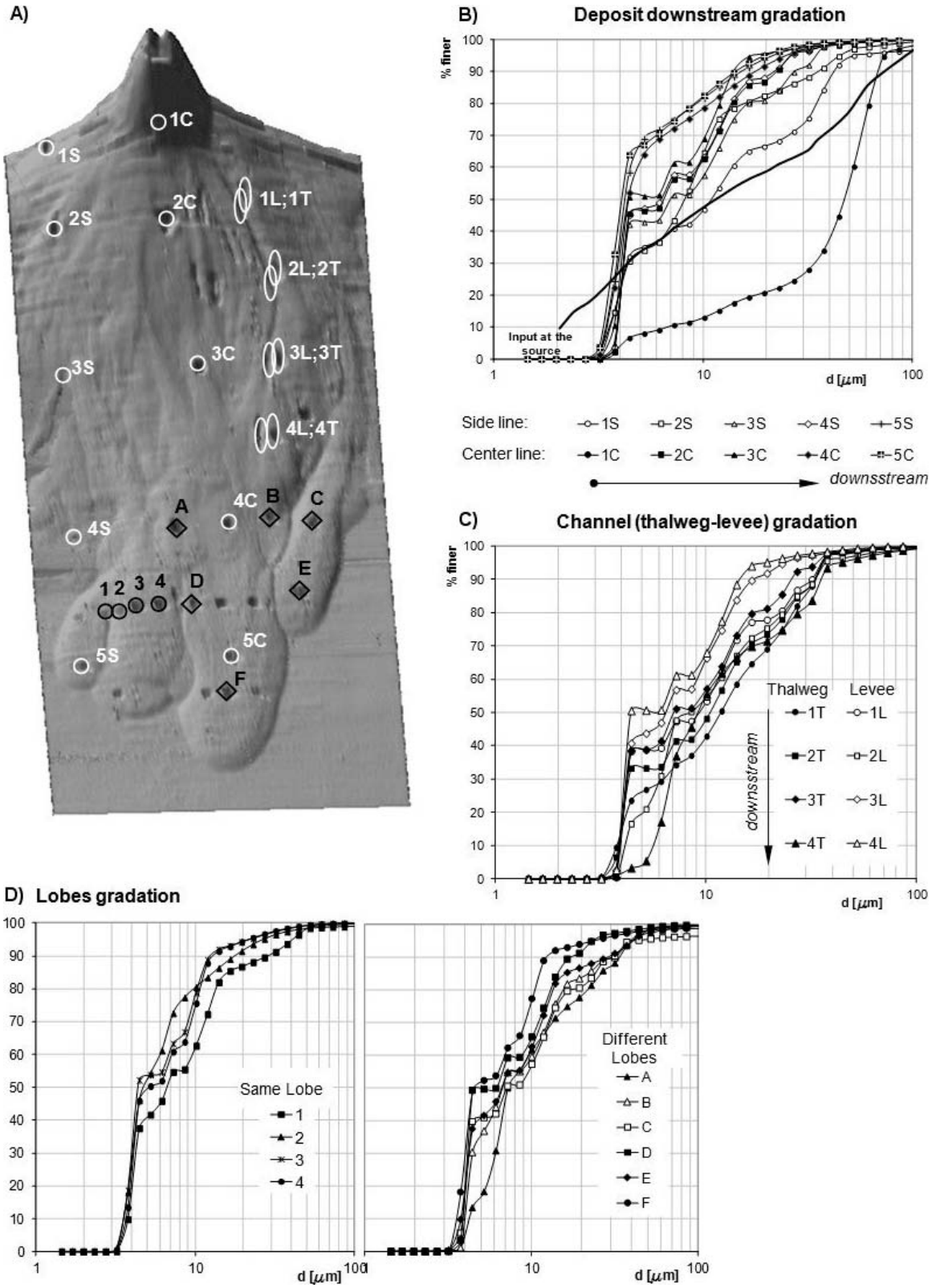

FIG. 12.—Patterns of grain-size variation of the deposit in *Experiment I-a*. **A)** Location of samples taken along the deposit. **B)** Grain-size variation along the deposit. **C)** Grain-size variation along channels (thalweg–levee). **D)** Grain-size variation along lobed features.

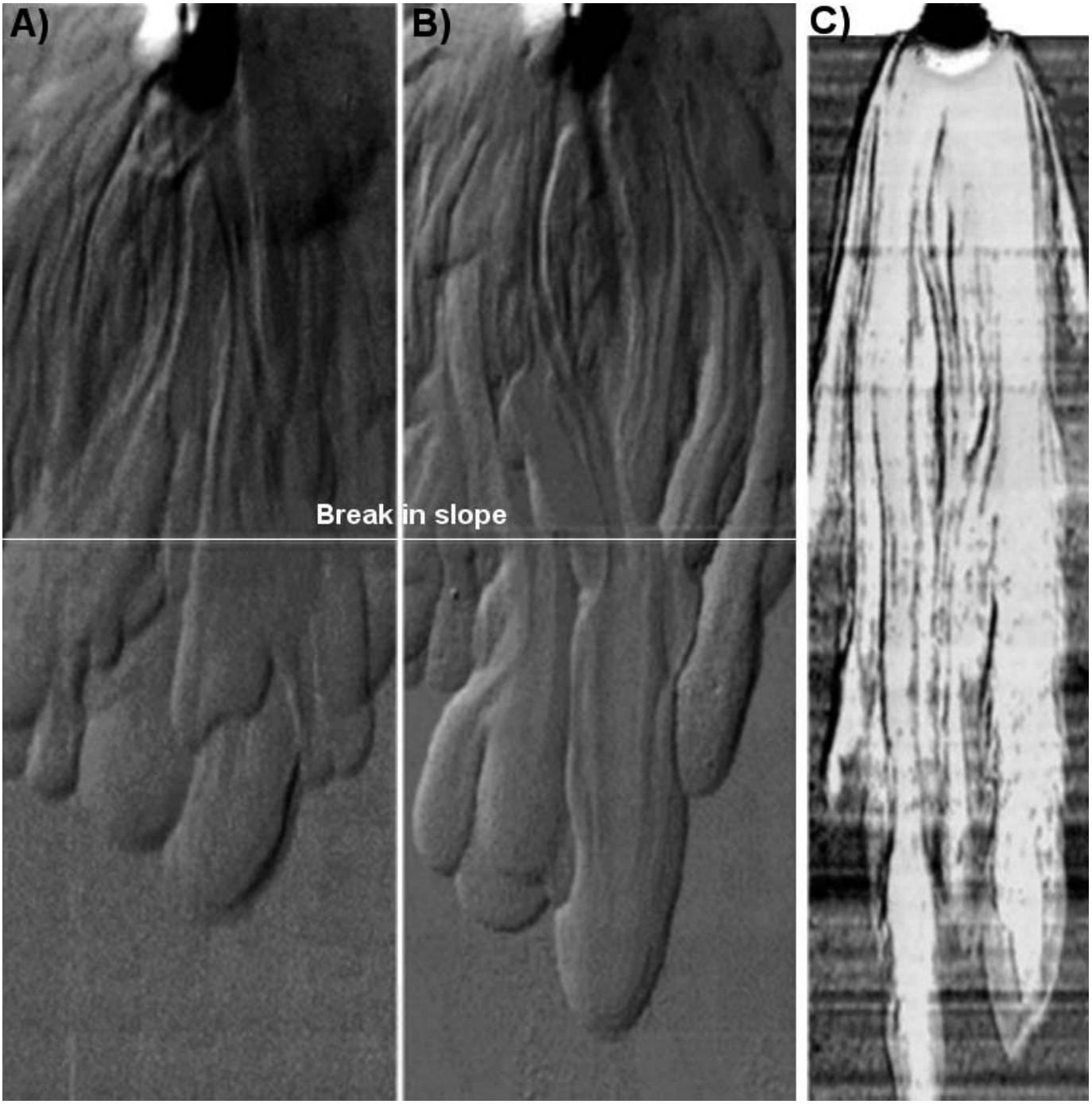

FIG. 13.—Comparison of deposits for different bed slope profiles: **A)** slope break from 0.07 to 0.025, **B)** slope break from 0.07 to 0.044, and **C)** constant slope of 0.07 (no slope break). The deposit shown in **A)** was 4 m long, in **B)** was 4.7 m long, and in **C)** 8 m long.

thalweg. The grain-size distributions illustrate: (a) an overall tendency for both channel and levee sediment to become finer downstream (with d_{50} declining from 12 μm at 1T to 8.5 μm at 4T and 45 μm at 1C to 4.3 μm at 4C), and (b) a tendency for levee sediment to be finer than channel sediment by about 4 μm (e.g., compare 4T and 4L).

Figure 12D shows grain size distributions within a single lobe (samples 1–4) and among lobes (samples A–F). The variation in grain-size distribution within a lobe is not strong. The upstream lobes A, B, and C, however, show somewhat coarser sediment than the downstream lobes D, E, and F.

ANALYSIS ON EFFECTS OF BREAK IN SLOPE ON FAN MORPHOLOGY

The basement slope break evident in Figure 1 played a very important role in governing sediment distribution, channel aggradation, and overall deposit architecture. Figures 3 and 9 show an intensely channelized middle-fan zone upstream of the basement slope break, and a zone of stacked lobes in the lower-fan zone downstream of the slope break. This change in behavior is likely due to the deceleration of the flow at the slope break, which encourages rapid deposition and inhibits the formation of leveed channels.

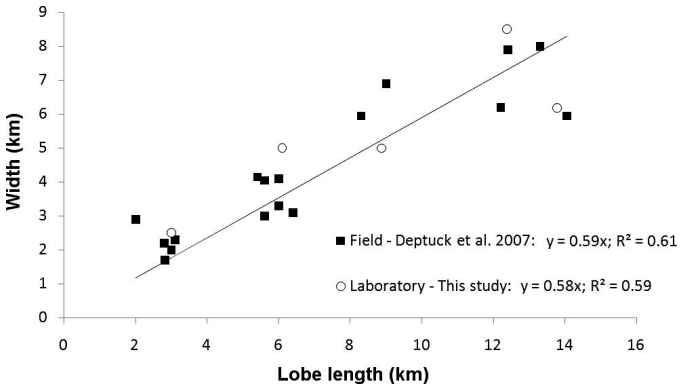

FIG. 14.—Here the lobe dimensions documented in Figure 8C have been upscaled by a factor of 10,000, in order to document aspect-ratio trends similar to the field data of Deptuck et al. (2007).

The auxiliary experiment *Experiment I-a* was performed in order to further explore the role of the basement slope break on fan morphology. Hence, *Experiment I-a* corresponds to *Experiment I* in all respects except lower basement slope.

Figure 13A and B documents the remarkable difference in bed topography at the end of these two experiments. Figure 13A, which corresponds to Figure 3H, shows a strongly channelized mid-fan region upstream of the break, and relatively short, fat lobes downstream of the break. Figure 13B, which corresponds to an increase in basement slope from 0.025 to 0.044, shows a considerable elongation of the lobes downstream of the slope break. The width of the lobes, however, is about the same.

The effect of having no slope break whatsoever is explored in Figure 13C. The experiment in question is that of Cantelli et al. (2011). It was conducted under conditions that are very similar to the ones reported here. It differs from *Experiment I* in that (a) the basement slope is everywhere equal to the upper basement value of 0.07 of *Experiment I*, (b) the volume concentration in the slurry is 0.10 rather than 0.05, (c) the slurry mixture includes a small component (5%) of 110 μm silica flour), and (d) the experiment consists of a larger number of runs with lower discharge than *Experiment I*.

These differences notwithstanding, Figure 13C allows documentation of the effect of having no slope break whatsoever. In contrast to Figure 13A and B, the channels extend more or less continuously downsteam, with only small, residual lobes at the end of each channel. It is evident from Figure 13 that a stronger slope break is associated with the formation of shorter and better defined lobes, and a weaker slope break is associated with long, continuous channels.

LOBE ASPECT RATIO

The issue of upscaling of results of experiments of the type described here to field scale is discussed in some detail in both Yu et al. (2006) and Cantelli et al. (2011). Figure 8 documents a tendency for lobe width to increase with lobe length in these laboratory experiments; the field data published in Deptuck et al. (2007) illustrates a similar trend. Figure 14 illustrates that when the experimental results are upscaled by a length scale factor λ of 10,000, the experimental data intermingle with the field data to illustrate a common trend. In the case of the present experiments, the basement slope break served as a driver for the formation of lobed features which display geometric similarity to those observed on natural basin floors (Fig. 14).

CONCLUSIONS

The laboratory work reported here pertains to subaqueous fans in the laboratory developing over a platform with a slope break, from high slope updip to low slope downdip. The experiments illustrate the morphodynamic evolution of laboratory channel–lobe systems. Their stratigraphy was reconstructed from sequential measurements of bed elevations.

The sediment-laden water entering the experimental tank formed a slurry, but the entrainment of ambient water quickly diluted the flow into a relatively dilute turbidity current. These turbidity currents were likely laminar, or at most weakly turbulent. At any given time, the turbidity current that could cover no more than a fraction of the platform, so that the focus of flow migrated or avulsed repeatedly across the fan surface. This created conditions for the formation, occupation, and abandonment of both channels and lobes.

The overall surface of the deposits showed three recognizable morphologic divisions from updip to downdip: (a) a steep sediment supply area defining the source zone of the fan; (b) a middle fan zone characterized by leveed channels; and (c) a lower zone beyond the basement slope break which was free of major channels, instead consisting of stacked depositional lobes. The last two of these three provide analogs for submarine channel-fan systems.

The slope break played a very important role in governing channel aggradation and overall architecture over the entire deposit. The middle fan was riddled with leveed channels, which would form spontaneously, be abandoned, and then form elsewhere. Although at any given time a single channel appeared to be dominant, more than this single channel was active. These weakly sinuous channels served to maintain optimum channel slopes to accommodate the volume of flow and sediment load in the channels. These channels were somewhat ephemeral in nature. While this feature may not be characteristic of the bulk of channelized submarine fans, it is characteristic of their distal regions (Yu et al. 2006; Cantelli et al. 2011). As fan gradient decreased downslope of the break in slope, channels subsequently developed a still weaker sinuosity, and then disappeared in favor of lobed features on the lower fan zone. The change in morphology was evidently mediated by flow deceleration caused by the slope break. This result suggests that channelization requires flow velocities above some threshold value.

These unchannellized lobes, which were much wider than their feeder channels updip, formed compensationally stacked deposits, reflecting avulsion of the feeder channels. The change to a gentle bottom gradient appeared to be more important than sediment-supply parameters (sediment load) in controlling the development of depositional lobes downdip of a slope break. This comment notwithstanding, a higher sediment feed rate resulted in more numerous lobes, each of a smaller size.

The results reported here are compared to an experiment of Cantelli et al. (2011), for which there was no slope break. In that experiment, no lobes formed, and the fan was channelized extensively, even far from the flow source. This observation provides further evidence for the role of a break in slope from high to low in mediating unchannelized lobe formation.

Bed sediment samples were chosen to characterize grain-size variation in channels, levees, and lobed feature along the deposit. The results document a clear downstream fining of the grain size material. They also document levees that contain finer sediment than the channels they bound.

Lastly, the comparison with field lobes analogs suggest a reasonable proportionality between dimensions, demonstrating that lobed fans can indeed be modeled, within limits, at laboratory scale. This observation provides one more illustration as to how small-scale, and indeed laminar morphodynamic processes, can create morphologies and stratigraphies that are remarkably similar to those observed at field scale (Paola et al. 2010; Lajeunesse et al. 2011).

ACKNOWLEDGEMENTS

Financial support which made these experiments possible was provided by Shell International Exploration and Production Inc., Houston, U.S.A. The

authors are very grateful to Dr. George Postma, Dr. Lawrence Amy, and Dr. William McCaffrey for their careful reading and helpful reviews of the manuscript.

REFERENCES

Baas, J.H., Van Kesteren, W., and Postma, G., 2004, Deposits of depletive high-density turbidity currents: a flume analogue of bed geometry, structure and texture: Sedimentology, v. 51, p. 1053–1088.

Cantelli, A., Pirmez, C., Johnson, S., and Parker, G., 2011, Morphodynamic and stratigraphic evolution of self-channelized subaqueous fans emplaced by turbidity currents: Journal of Sedimentary Research, v. 81, p. 233–247.

Deptuck, M., Piper, D., Savoye, B., and Gervais, A., 2007, Dimensions and architecture of late Pleistocene submarine lobes off the northern margin of East Corsica: Sedimentology, v. 55, p. 869–898.

Gray, T., Alexander, J., and Leeder, M., 2005, Quantifying velocity and turbulence structure in depositing sustained turbidity currents across breaks in slope: Sedimentology, v. 52, p. 467–488.

Imran, J., Parker, G., and Katapodes, N., 1998, A numerical model of channel inception on submarine fans: Journal of Geophysical Research, v. 103, p. 1219–1238.

Imran, J., Parker, G., and Harff, P., 2002, Experiments on incipient channelization of submarine fans: Journal of Hydraulic Research, v. 40, p. 21–32.

Lajeunesse, E., Malverti, L., Lancien, P., Armstrong, L., Métivier, F., Coleman, S., Smith, C.E., Davies, T., Cantelli, A., and Parker, G., 2010, Fluvial and subaqueous morphodynamics of laminar and near-laminar, flows: a synthesis: Sedimentology, v. 57, p. 1–26.

Métivier, F., Lajeunesse, E., and Cacas, M., 2005, Submarine canyons in the bathtub: Journal of Sedimentary Research, v. 75, p. 6–11.

Mulder, T., and Alexander, J., 2001, Abrupt change in slope causes variation in the deposit thickness of concentrated particle-driven density currents: Marine Geology, v. 175, p. 221–235.

Neethling, J.M., 2009, Stratigraphic Evolution and Characteristics of Lobes: a High-Resolution Study of Fan 3, Tanqua Karoo, South Africa [M. Sc. Thesis]: Stellendbosch University, 72 p.

Ouchi, S., Ethridge, F., James, E., and Schumm, S., 1995, Experimental study of subaqueous fan development, *in* Hartley, A., and Prosser, D., eds., Characterization of Deep Marine Clastic Systems: Geological Society of London, Special Publication 94, p. 13–29.

Paola, C., Straub, K.M., Mohrig, D.C., and Reinhardt, L., 2009, The "unreasonable effectiveness" of stratigraphic and geomorphic experiments: Earth-Science Reviews, v. 97, p. 1–43.

Parsons, J.D., Scheller, W., Stelting, C., Southard, J., Lyons, W., and Grotzinger, J., 2002, A preliminary experimental study of turbidity fan deposits: Journal of Sedimentary Research, v. 72, p. 619–628.

Pirmez, C., 1994, Growth of a Submarine Meandering Channel Levee System on Amazon Fan [Ph.D. Thesis]: New York, Columbia University, 587 p.

Yu, B., Cantelli, A., Marr, J., Pirmez, C., O'Byrne, C., and Parker, G., 2006, Experiments on self-channelized subaqueous fans emplaced by turbidity currents and dilute mudflows: Journal of Sedimentary Research, v. 76, p. 889–902.

Received 30 September 2012; accepted 12 August 2013.